

# Supporting Information for "First principles based screen for identification of transparent conductors"

Yuwei Li<sup>†,‡</sup> and David J. Singh<sup>\*,‡</sup>

*North China Institute of Aerospace Engineering, No. 133 Aimin East Road , Langfang, Hebei 065000, China, and Department of Physics and Astronomy, University of Missouri, Columbia, MO 65211-7010 USA*

E-mail: singhdj@missouri.edu

---

\*To whom correspondence should be addressed

†North China Institute of Aerospace Engineering, No. 133 Aimin East Road , Langfang, Hebei 065000, China

‡Department of Physics and Astronomy, University of Missouri, Columbia, MO 65211-7010 USA

Table S1: The optical and electrical fitness function (*OEF*) of the wide bandgap semiconductors considered. All materials are calculated for p-type, except  $\text{In}_2\text{O}_3$ , which is shown for n-type.

	<i>OEF</i>			
	solar		PV	
	$10^{20} \text{ cm}^{-3}$	$10^{21} \text{ cm}^{-3}$	$10^{20} \text{ cm}^{-3}$	$10^{21} \text{ cm}^{-3}$
BP	12.47	14.93	16.98	21.18
ZnS	13.01	14.61	17.73	20.61
MgS	11.95	14.35	16.26	20.56
MgTe	14.38	13.36	18.50	21.20
$\text{B}_6\text{O}$	12.44	13.17	16.90	19.30
ZnSe	13.03	12.07	8.56	20.50
BeTe	13.89	11.36	18.69	20.51
$\text{La}_2\text{O}_2\text{Te}$	6.52	11.24	0.24	8.38
GaSe	8.14	10.92	2.51	14.83
ZnTe	9.35	8.91	1.02	18.18
$\text{Al}_2\text{Se}_3$	7.34	8.28	9.97	10.71
$\text{Ba}_2\text{BiTaO}_6$	10.24	8.07	12.55	9.68
$\text{CsLaO}_2$	7.46	7.87	13.36	16.43
$\text{AgLaO}_2$	5.85	7.11	6.89	9.53
$\text{La}_2\text{O}_2\text{Se}$	6.56	6.41	6.76	6.40
$\text{BrLaO}_2$	6.17	6.25	8.54	8.36
$\text{AgYS}_2$	4.31	5.54	0.24	4.79
$\text{Cs}_2\text{Zn}_3\text{Te}_4$	5.61	5.42	2.54	7.15
$\text{CuAlO}_2$	5.23	5.31	4.81	4.73
$\text{AgAlO}_2$	4.57	4.96	0.22	1.45
KYS <sub>2</sub>	6.00	4.76	14.10	12.99
$\text{Cs}_2\text{Zn}_3\text{Se}_4$	4.95	4.68	6.44	4.18
$\text{CaPb}_2\text{O}_3$	3.77	3.79	5.37	5.76
$\text{SrPb}_2\text{O}_3$	3.33	2.71	4.26	3.67
$\text{BaPbO}_2$	2.98	2.62	4.02	3.93
$\text{Pr}_2\text{SeO}_2$	1.20	2.60	0.11	0.69
$\text{BaPb}_2\text{O}_3$	2.09	1.96	2.51	2.45
$\text{In}_2\text{O}_3$	14.40	14.78	20.27	20.85

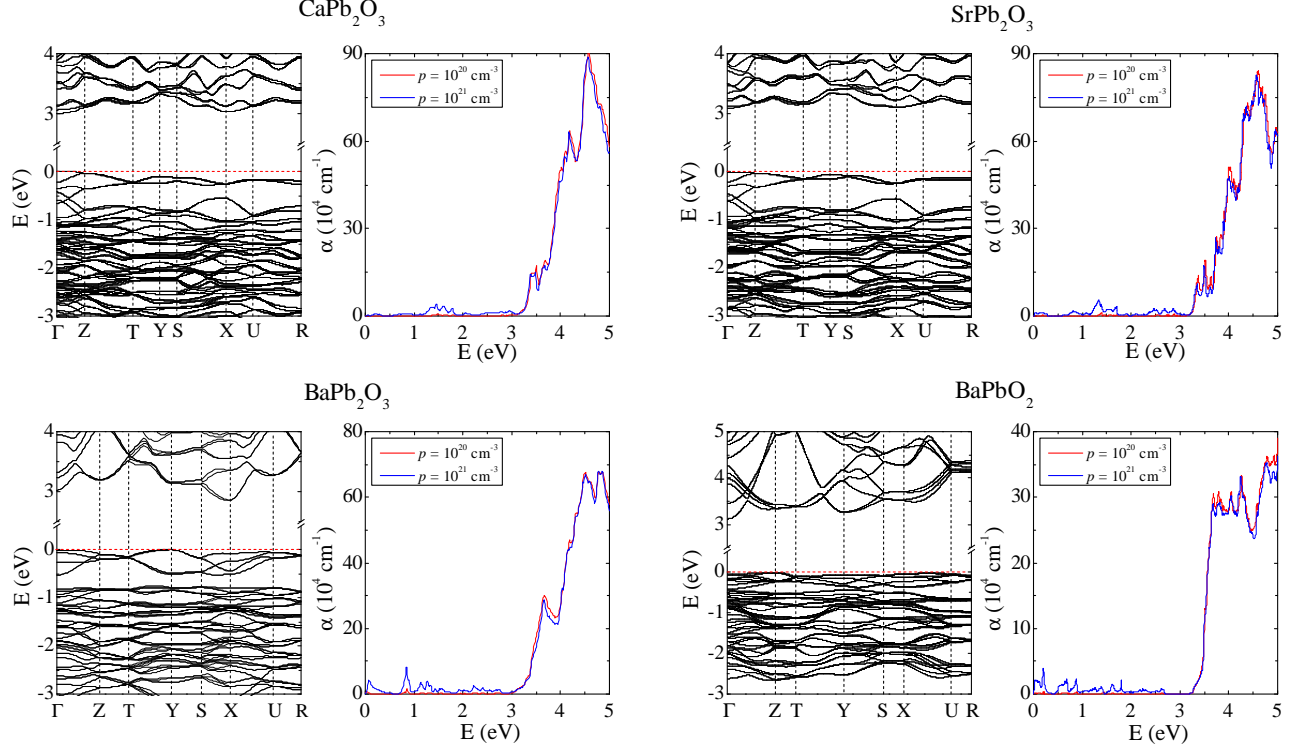


Figure S1: The band structures and absorption spectra of  $\text{CaPb}_2\text{O}_3$ ,  $\text{SrPb}_2\text{O}_3$ ,  $\text{BaPb}_2\text{O}_3$  and  $\text{BaPbO}_2$  respectively. The valence band maximum is set to energy zero.

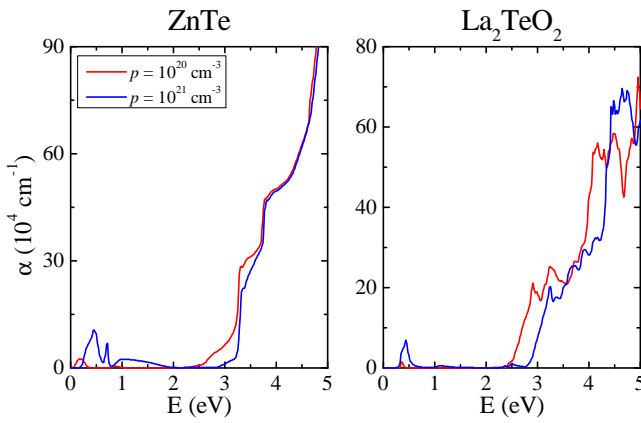


Figure S2: The absorption spectra of  $\text{ZnTe}$  and  $\text{La}_2\text{TeO}_2$  respectively.

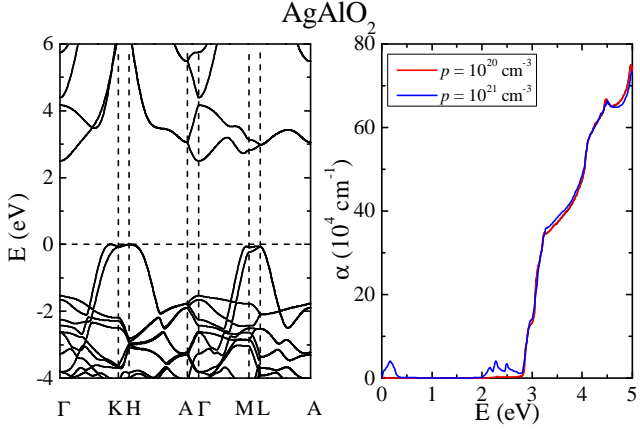


Figure S3: The band structure and absorption spectrum of  $\text{AgAlO}_2$ . The valence band maximum is set to energy zero.

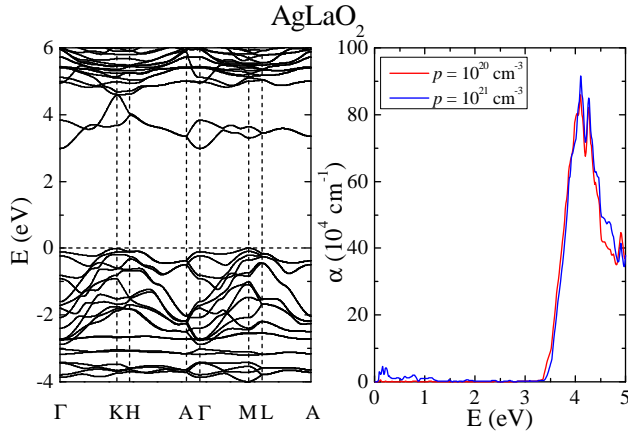


Figure S4: The band structure and absorption spectrum of  $\text{AgLaO}_2$ . The valence band maximum is set to energy zero.

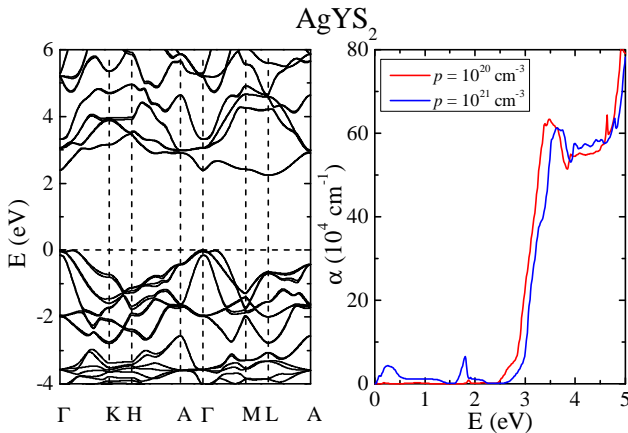


Figure S5: The band structure and absorption spectrum of  $\text{AgYS}_2$ . The valence band maximum is set to energy zero.

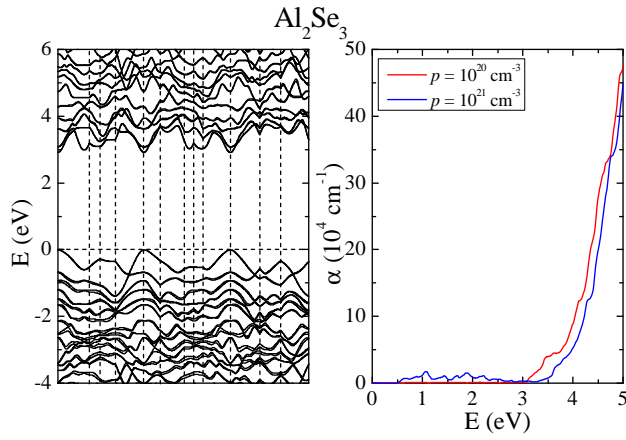


Figure S6: The band structure and absorption spectrum of  $\text{Al}_2\text{Se}_3$ . The valence band maximum is set to energy zero. Band structure path: (0.00, 0.00, 0.00) - (0.50, 0.00, 0.00) - (0.54, -0.04, 0.26) - (0.40, -0.04, 0.40) - (0.00, 0.00, 0.00) - (-0.10, 0.64, -0.10) - (0.40, 0.23, -0.00) - (0.50, -0.00, -0.00) - (0.63, -0.27, 0.27) - (0.00, 0.00, 0.00) - (0.27, 0.50, -0.27) - (-0.10, 0.64, -0.10) - (0.40, -0.04, 0.40).

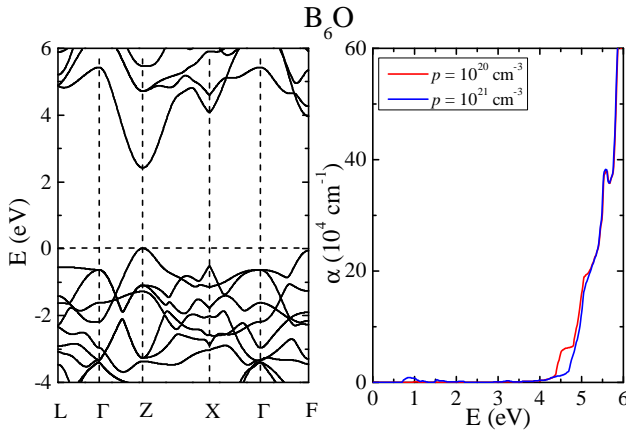


Figure S7: The band structure and absorption spectrum of  $\text{B}_6\text{O}$ . The valence band maximum is set to energy zero.

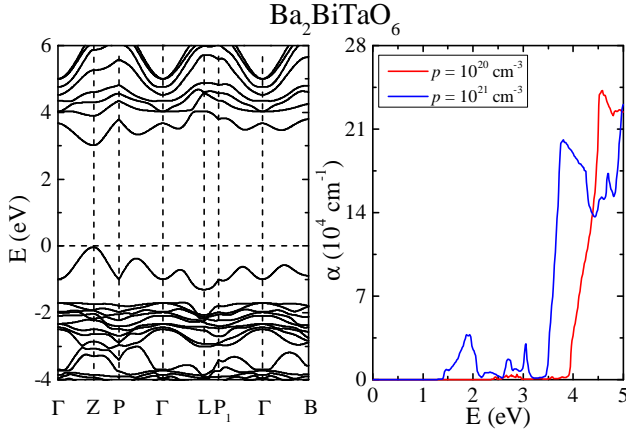


Figure S8: The band structure and absorption spectrum of  $\text{Ba}_2\text{BiTaO}_6$ . The valence band maximum is set to energy zero.

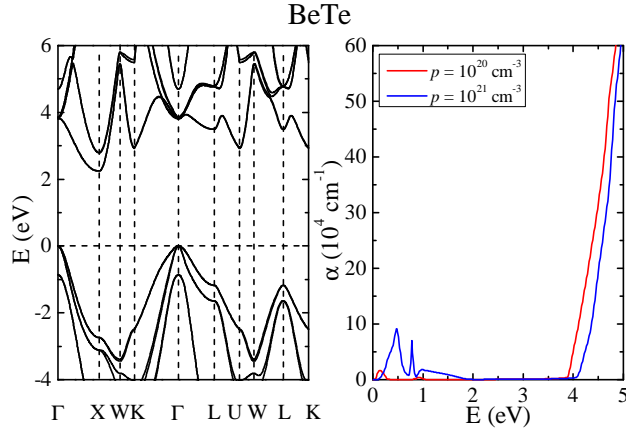


Figure S9: The band structure and absorption spectrum of BeTe. The valence band maximum is set to energy zero.

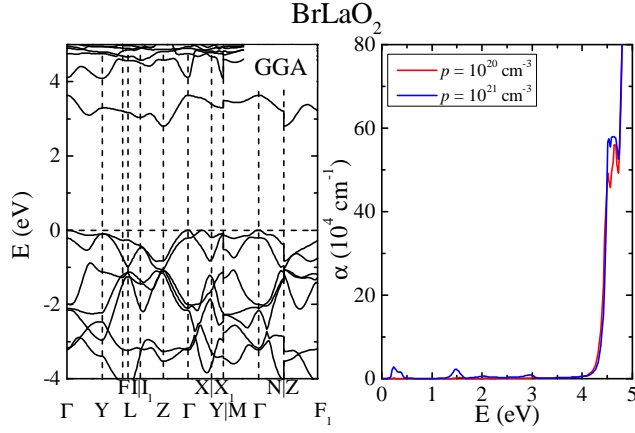


Figure S10: The band structure and absorption spectrum of  $\text{BrLaO}_2$ . The band structure is calculated using VASP code with the generalized gradient approximation of Perdew, Burke and Ernzerhof (PBE-GGA). The valence band maximum is set to energy zero.

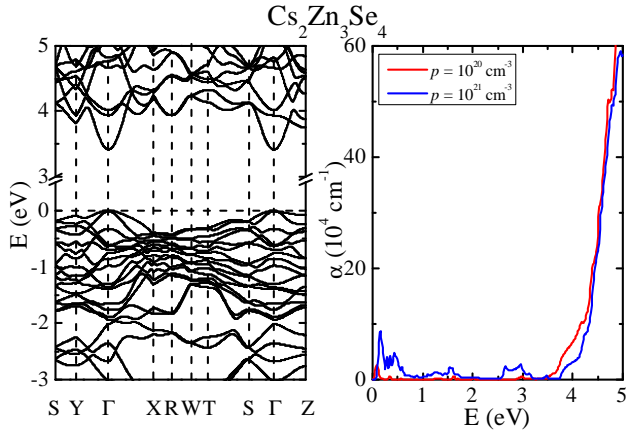


Figure S11: The band structure and absorption spectrum of  $\text{Cs}_2\text{Zn}_3\text{Se}_4$ . The valence band maximum is set to energy zero.

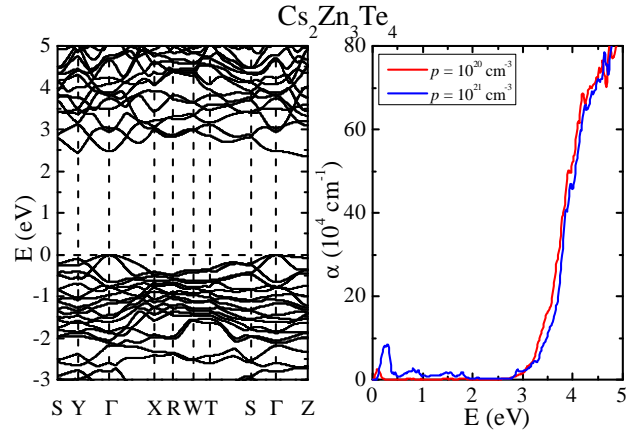


Figure S12: The band structure and absorption spectrum of  $\text{Cs}_2\text{Zn}_3\text{Te}_4$ . The valence band maximum is set to energy zero.

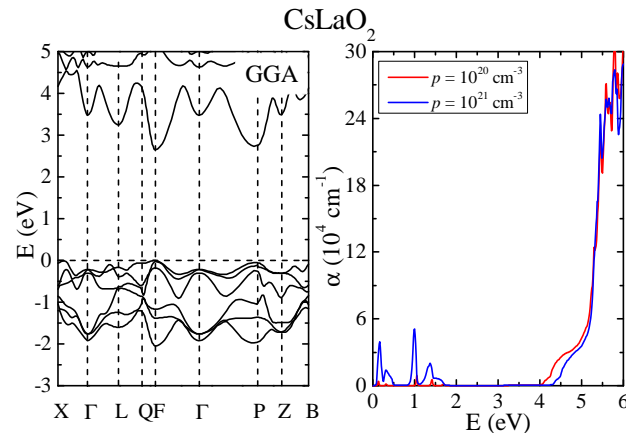


Figure S13: The band structure and absorption spectrum of  $\text{CsLaO}_2$ . The band structure is calculated using VASP code with the PBE-GGA functional. The valence band maximum is set to energy zero.

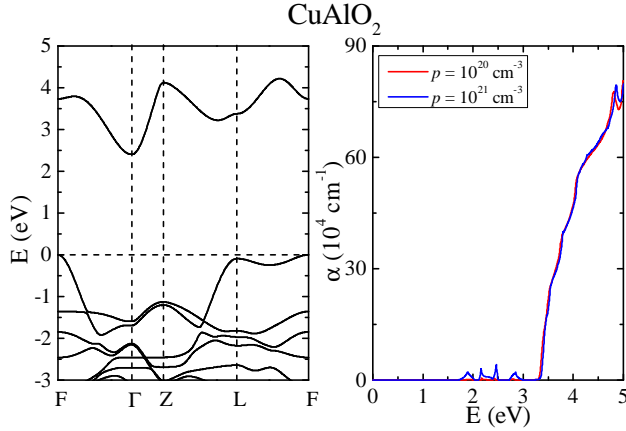


Figure S14: The band structure and absorption spectrum of CuAlO<sub>2</sub>. The valence band maximum is set to energy zero.

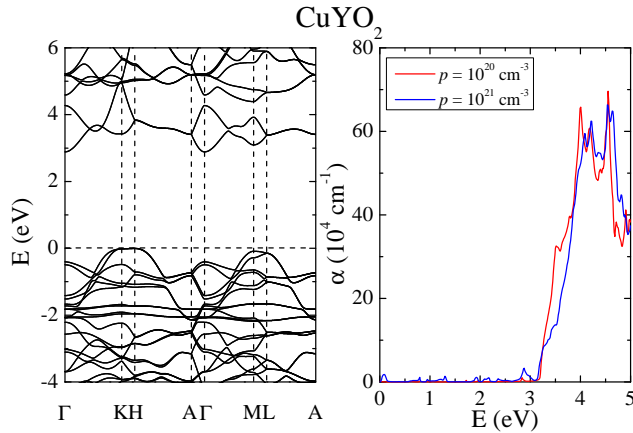


Figure S15: The band structure and absorption spectrum of CuYO<sub>2</sub>. The valence band maximum is set to energy zero.

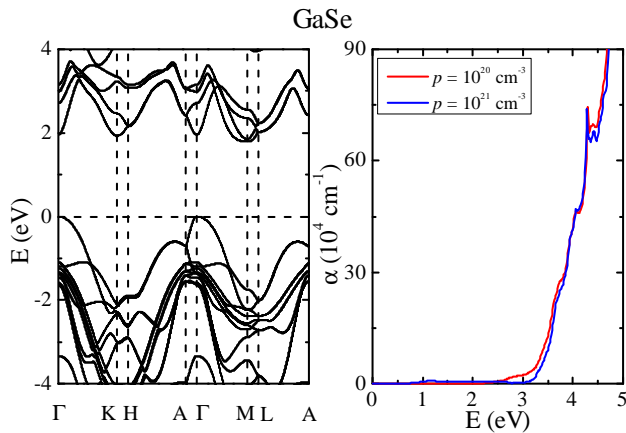


Figure S16: The band structure and absorption spectrum of GaSe. The valence band maximum is set to energy zero.

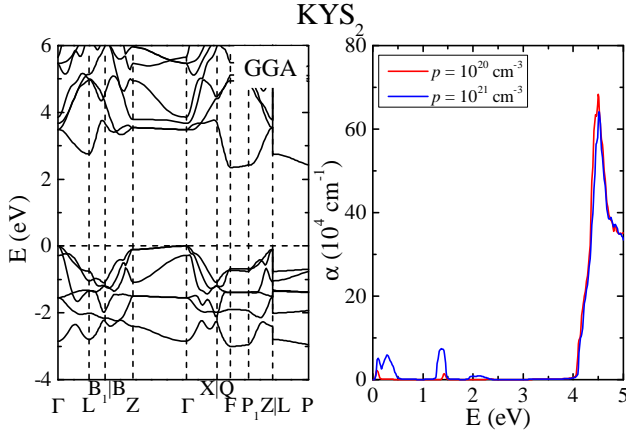


Figure S17: The band structure and absorption spectrum of  $\text{KYS}_2$ . The band structure is calculated using VASP code with the PBE-GGA functional. The valence band maximum is set to energy zero.

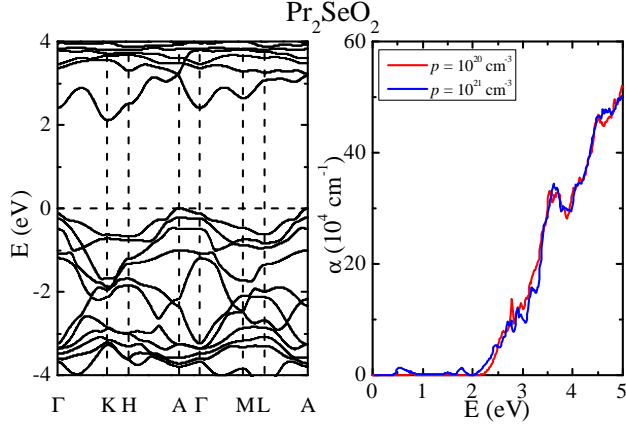


Figure S18: The band structure and absorption spectrum of  $\text{Pr}_2\text{SeO}_2$ . The valence band maximum is set to energy zero.

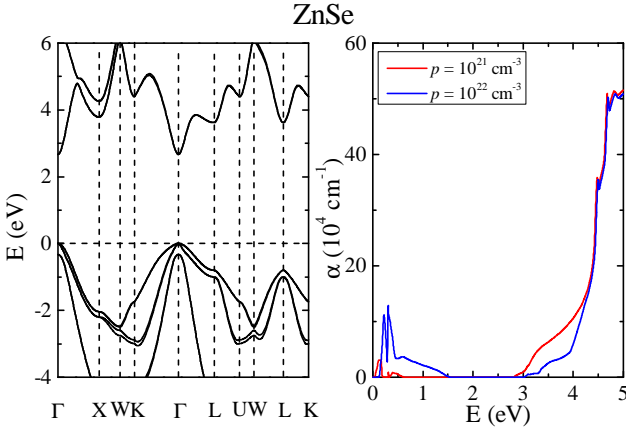


Figure S19: The band structure and absorption spectrum of  $\text{ZnSe}$ . The valence band maximum is set to energy zero.